Purging Research of Proton Exchange Membrane Fuel Cell at Low Temperature

Hailan Zhao

Abstract—**Low-temperature purge significantly impacts the performance of Proton Exchange Membrane Fuel Cell (PEMFC) under cold start condition. To explore the influence of gas blowing on PEMFC at low temperature, first of all, a three-dimensional and multiphase-physical model for a single cell is established. Secondly, the performance impacts of two factors, the water content in proton exchange membrane and the ambient temperature, on PEMFC are analyzed. Then, the influences of gas flow rate, blowing time and gas temperature on water content in membrane are conducted. The results indicate that a higher initial water content in the membrane at a lower start-up temperature shortens the duration of the cold start process. Consequently, it leads to increase cold starting failures. As the gas flow rate increases, the water content in the membrane decreases as the change rate decreases. The water content can be reduced by extending the purging time, but beyond a certain threshold no significant change is observed. Furthermore, the purge gas temperature shows minimal impact on the rate of change of water content. However, as it increases, the water content decreases. In order to balance both the purging effect and energy consumption, the purging flow rate of 1×10^{-5} kg.s^{-1} and the purging time of 56 seconds are recommended.**

Index Terms—**PEMFC, Cold Start, Gas Purge, Water Content in Membrane**

I. Introduction

The development and deployment of fuel cell are pivotal for mitigating global carbon emission[1]. As PEMFC shows significant advantages, operating at ambient temperature with high energy density, substantial specific power and excellent efficiency, it has great application prospect in automotive industry[2,3]. The major challenge of its application is the cold-start performance under freezing temperature. The process is complicated by the formation of ice at the cathode. Specially, the ices obstruct both the catalytic reaction interface and the gas channel[4], potentially leading to startup failure if the effective reaction temperature is lower than and the ice covers the catalytic layer[5]. Low-temperature purging plays a crucial role in ensuring the success start of PEMFC under freezing temperature[6]. Therefore, studying the effect of purging on the cold start of PEMFC is of great importance for the safe and reliable utilization.

The heating rate and the ice-formation rate have significant impact on the low-temperature performance. The dynamic balance between the two factors is the key to success of cold start[7]. The initial water content in the membrane significantly influences both the rate and extent of ice formation. Therefore, the expulsion of water through purging is an essential step in low-temperature startup. Purging water is a process of gaseous material transport[8]. Current methods focusing on the influence of purging on cold start are categorized into experimental test and simulation analysis [9-11]. For instance, S. Lee et al. explored the impacts of purge time, gas flow rate and reactor temperature on the internal water content of PEMFC through experiment[12]. Although experimental approach provides highly accurate data, it is limited in its ability to analyze cold-start performance in real-time under varying conditions, such as various temperatures and gas humidity. Furthermore, this method is also constrained by experimental setups. Simulation analysis allows for the exploration of cold start performance under diverse operations with a low cost. P. Xu, et al. established a one-dimensional water transfer model for purging and water removal. The effects of initial cell temperature, purge gas flow rate, anode purge gas and other parameters on internal water content are investigated[13]. M. Luo, et al., by using secondary purge of dry air, conducted the water removal from PEMFC. The changes in water content and internal resistance influenced by purge are obtained[14]. However, as the one-dimensional model is unable to confirm the influence of spatial variations, such as water content and air distribution within the PEMFC, the precision of numerical simulation is limited by the one-dimensional model.

In summary, to balance the cost-efficiency and analytical precision, a three-dimensional multi-phase physical model is constructed with validation. On this basis, the influences of water content in membrane and ambient temperature on cold-start capability are studied. Furthermore, the effects of purge flow rate, purge time and purge gas temperature on water content of membrane are analyzed.

Manuscript received September 16, 2023; revised September 24, 2024. This work was supported in part by the Major Innovation Projects in Shandong under Grant 2020CXGC010405 and 2020CXGC010406, the Innovation team project of "Qing-Chuang science and technology plan" of colleges and universities in Shandong Province 2021KJ083, the National Natural Science Foundation Project of China under Grant 52102465, the Postdoctoral Science Foundation of China and Shandong under Grant 2020M680091 and 202003042.

Hailan Zhao is a lecturer of Zibo Vocational Institute, Zibo, 255300 PR China. (e-mail: 12102@zbvc.edu.cn).

II. PEMFC Modeling

A. Transport model of water in membrane

(1) Electroosmosis-drag model

Electroosmosis-drag means the phenomenon that, when a proton migrates from anode to cathode across membrane, a defined number of water molecules transfer together with it.

This migration results in the translocation of water from anode to cathode . During this process, protons traverse in the form of hydrated hydrogen ions, which signifies that they are enveloped by water molecules. Consequently, the electroosmosis-drag coefficient is defined as the number of water molecules transported per mole of proton migration. The water flux across the membrane due to electroosmosis drag is quantified as follows:

$$\lambda_{mw,EOD} = n_d \frac{J_{(H^+)}}{F} \tag{1}$$

Where, $\lambda_{\mathrm{mw,EOD}}$ is the transmembrane flux of the transported water dragged by electroosmosis. n_{d} is the electroosmosis-drag coefficient. $J_{(\mathrm{H+})}$ is the current density of proton migration.

(2) Concentration diffusion

Concentration diffusion refers to the movement of molecules driven by the gradient in water concentration within electrolyte. As the electrochemistry reaction at cathode generates water, the concentration of water at cathode exceeds than that at anode. Consequently, concentration diffusion happens from cathode toward anode. This mechanism helps to alleviate disparities in water distribution. The water flux caused by concentration diffusion is expressed as follows:

$$\lambda_{mw,diff} = -\frac{\rho m}{EW} D_{mw} \nabla \lambda \tag{2}$$

Where, $\lambda_{\mathrm{mw,diff}}$ is the flux of water caused by concentration diffusion. D_{mw} is the diffusion coefficient of water in electrolyte. λ is the water content in the electrolyte. ρ_{m} is the dry film density. EW is the equivalent mass of membrane. The negative sign indicates that the direction of diffusion flux is along the direction of concentration decrease.

(2) Hydraulic penetration

Hydraulic penetration refers to the osmotic action of water movement driven by pressure gradient. The flux of water permeated by hydraulic is shown below.

$$\lambda_{mw,hyd} = -\lambda \frac{\rho m}{EW} \cdot \frac{K_{mw}}{\mu_{lq}} \nabla P_{mw} \tag{3}$$

Where, $\lambda_{\mathrm{mw,hyd}}$ is the flux of water across the membrane caused by hydraulic permeation. P_{mw} is the hydraulic pressure in electrolyte. μ_{lq} is the viscosity of liquid water. K_{mw} is the permeability coefficient of membrane to liquid water. The negative sign preceding the expression indicates that the direction of the diffusion flux decreases with increasing concentration.

Due to the low permeability of membrane, when the intake pressures at cathode and anode are equal, the water flux from the pressure difference is much lower than that from concentration diffusion and electroosmotic drag.

B. Substance transport model

(1) Darcy law

The properties of a porous medium significantly influence fluid flow within it. Laminar flow through a porous medium can be accurately described by Darcy law, which assumes that other forces are negligible[15].

$$\nabla P = -\frac{\mu}{K} \vec{u} \tag{4}$$

Where, μ is the dynamic viscosity. K is the permeability coefficient. $\vec{u}$ is the velocity vector.

The gas permeability is as following.

$$K_g = K_0 (1 - \frac{v}{q})^3 \tag{5}$$

Where, K_{g} is the gas permeability coefficient. K_0 is the permeability coefficient of the material.

The permeability coefficient of liquid is as following.

$$K_{lq} = K_0 v_{lq}^{\ 3} \tag{6}$$

Where, K_{lq} is the permeability coefficient of liquid.

(1) Fick Law

Considering the convection and diffusion of material components in PEMFC, the diffusion transport of each material component can be described, by using Fick law in a broad sense[16].

$$\frac{\partial(\varepsilon C)}{\partial t} + \nabla(\varepsilon \vec{u} C) = \nabla(D_i^{eff} \nabla C) + S_i \tag{7}$$

Where, the left two items are the unsteady state term and the convective term. The right two are the diffusion term and the diffusion source term. C is the component concentration. $\vec{u}$ is the velocity vector.

C. Three-dimensional numerical model

The three-dimensional solid model of PEMFC constructed in this study is segmented into nine sections. As shown in figure 1, arranged from exterior to interior, the sections include cathode and anode bipolar plates, flow channels, diffusion layers, catalytic layers and the proton exchange membrane. The model features a single serpentine runner discretized by meshing technique. Given the variation in thickness of the proton exchange membrane and catalytic layers which range from tens to over a hundred microns, meticulous refinement of the mesh is of great importance in these regions.

The mesh function plays as a control volume framework, where each element is interconnected by nodes. The simulation process entails solving equations for each control volume to ensure the accuracy. The model comprises a total of 1,440,000 mesh elements, distributed among 960,000 grids in fluid computation areas. It has 480,000 grids in solid computation areas and 1,677,283 nodes, which facilitate a detailed and robust simulation environment.

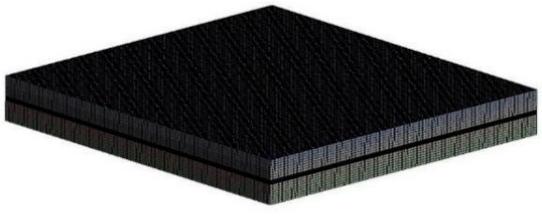

Fig. 1 Mesh of PEMFC model

D. Model Validation

Table 1 gives the operating parameters for the model of single PEMFC. Furthermore, startup with a constant voltage, 0.6V, is set in the model, to simulate the performance of PEMFC.

Table 1 Operating parameters of PEMFC

Parameter name	Value	Parameter name	Value
Open circuit voltage /V	0.95	Relative humidity	0.5
Inlet temperature/℃	27	Runner entrance area /cm^2	0.01
Operating pressure/kPa	101.33	Reference current density of anode /$A.m^{-2}$	10000
Stoichiometry ratio between cathode and anode	2:1.5	Reference current density of cathode /$A.m^{-2}$	20

Based on the iterative calculation of the model, the temperature distribution of the PEMFC is obtained as shown in figure2. The result shows that the average temperature of the PEMFC is about 81.68℃. The region with the highest temperature is located at the catalytic layer of cathode. The region of runner inlet shows the lowest temperature. The distribution of the PEMFC temperature is uniform. Thus, the model is suit for the performance study of the PEMFC.

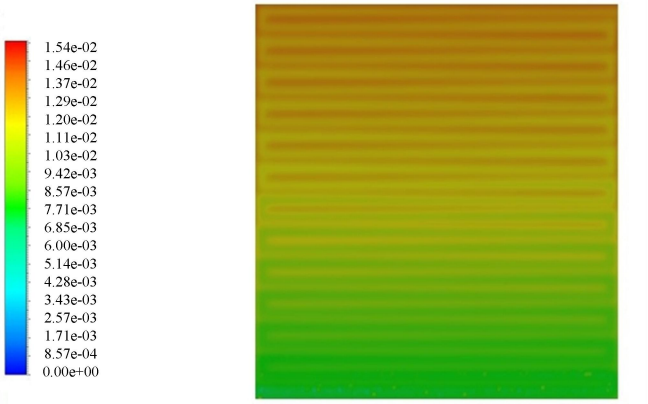

Fig. 2 Temperature distribution of PEMFC under given conditions

Current density is an important indicator for the performance of PEMFC. According to the electrochemical reaction principle of PEMFC, the current density distribution of PEMFC is similar to the distribution of reaction-generated water. The relationship between current density and rate of water production is shown as following.

$$q_{H_2O} = M_{H_2O} \frac{J}{2F} \tag{8}$$

Where, q_{H2O} is the rate of water generation. M_{H2O} is the molar mass of water. J is the current density. F is the Faraday coefficient.

The distributions of current density and water molar concentration in PEMFC are confirmed as shown in figure 3 and figure 4. According to the results, as the electrochemical reaction proceeds, both the current density and water molar concentration gradually increase along the direction of gas flow. Stronger electrochemical reaction is obtained in the middle section of PEMFC. In the front section, due to the higher ohmic polarization caused by the lower water content in the membrane, the electrochemical reaction is weakest. In the rear section, as a result of the consumption of reaction gas and the decrease of fuel participating in the reaction, the electrochemical reaction is relatively weak.

Fig. 3 Distribution of current density in PEMFC

Fig. 4 Distribution of water molar concentration in PEMFC

Water inside the PEMFC primarily originates from the electrochemical reaction and the moisture carried by reaction gases. The transport of water in the proton exchange membrane is dominated by back-diffusion from cathode to anode at low current density. While the current density is high, it is primarily driven by electroosmotic drag from anode to cathode. When the effect of the two mechanisms reach equilibrium, the water content in the membrane reaches the optimal state. In the cathode side, the water produced by the reaction not only diffuses back to anode but also is absorbed by proton exchange membrane and porous media. Additionally, a portion of the water is blown away by the unreacted gas. The water that remains in the porous media prolongs the low-temperature startup time.

To verify the simulation model, a performance test platform for PEMFC is constructed as shown in figure 5. The test system consists of electronic load, PEMFC, low-pressure hydrogen gas bottle and upper management system. The electronic load is used for consuming the current generated by PEMFC. The low-pressure gas bottles are used to reduce storage capacity of hydrogen to ensure the safety of experiment. The upper management system is designed for data collection and processing. The control system is able to automatically collect and process data, regulate the intake of fuel gas and perform hydrothermal management. Furthermore, based on the upper management system, the performance data of a single-chip PEMFC can be obtained to verify the simulation model proposed above.

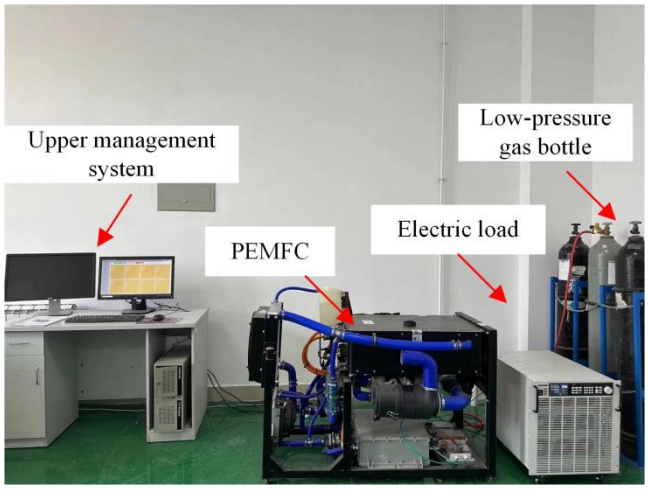

Fig. 5 Test platform for PEMFC

As depicted in figure 6, a comparative analysis of polarization curves between the experiment and simulation data of PEMFC is given. Results reveal that the simulation data slightly exceeds the experiment data within the low to medium current density ranges. The overall trends remain largely consistent across higher current densities, where the discrepancy between the two results becomes more pronounced. This divergence is primarily attributed to the experiment conditions. As the temperature of PEMFC gradually increases, it enhances the electrochemical reactions, leading to the increase of water production. Such accumulation of water in the catalytic layer hampers the electrochemical reaction process. In contrast, the numerical simulation operates under ideal conditions for all components, which accounts for the higher current density. Despite these discrepancies, the error margin of the simulation model is maintained within 3%, it satisfies the analytical requirement.

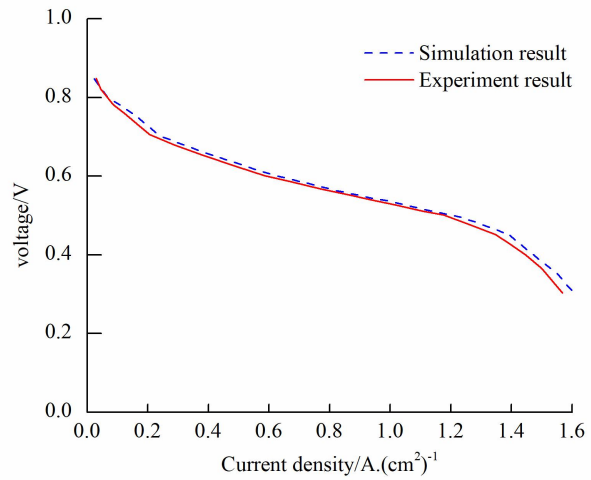

Fig. 6 Polarization curves of PEMFC between simulation and experiment results

III. Analysis of the Effect of Water Content in Membrane and Start-up Temperature on Low-temperature Startup

A. Analysis of the Purging and Dewatering Process

The influence of ambient temperature on the purging and dewatering process of PEMFC can be confirmed by changing the temperature of purging gas. Higher ambient temperature means faster purging process. Research has confirmed that the optimal purging effect can be obtained when the ambient temperature is 80°C[17,18]. Therefore, in this paper, the ambient temperature of PEMFC under shutdown condition is controlled around 80°C. As for the type of purging gas, compared with dry air, dry hydrogen has superior dewatering capability. However, this method will consume larger amount of hydrogen, thereby increases the cost of use. Furthermore nitrogen shows greater safety on the purging process. Nevertheless, the compact layout of vehicle makes it difficult to accommodate additional space for a nitrogen tank. Given the above analysis, dry air is used as the purging gas. It is used as the medium for purging by the air supply system to blow the PEMFC under shutdown operation.

The moisture in PEMFC is carried away by high-speed gas flow in the channels through evaporation, diffusion and convection. Thus, when the stack temperature drops to the same level as ambient temperature, the purging time needs to be doubled to dry the stack. Therefore, the purging and dewatering process should be carried out immediately after shutdown. It should be noted that, constant-voltage startup have an advantage over constant-current startup only when the PEMFC has been dried with sufficient dry air.

According to figure 7, the high-speed gas passes through the gas channels firstly and blows away the water vapor and small droplets within the channels. Then, the liquid water within the diffusion layer is transferred to the gas channel through evaporation and capillary force action, where it is blown away by the high-speed gas. The evaporation process of the liquid water in the diffusion layer is similar as a process, where an evaporation interface continuously moves inward. Using the evaporation interface as a reference, the area in front of the interface maintains its original liquid water content, while the area behind it becomes a dry zone after purging.

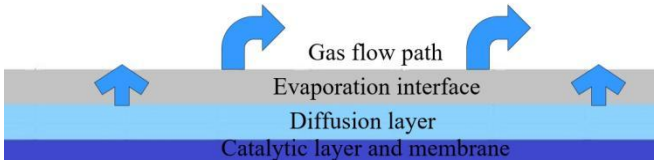

Fig. 7 Purging and dewatering process in PEMFC

When the evaporation interface reaches the catalyst layer, the liquid water in the diffusion layer has been completely blown away. Upon reaching the catalyst layer, the purging process differs from that in the diffusion layer. The liquid water in the catalyst layer has two types. One is the liquid water in the pores. The other one is the membrane water in the ion-conducting polymer. Similar to diffusion layer, the purging and dewatering process in catalyst layer involves evaporation and diffusion under capillary force action. However, the amount of water that can be blown away in the catalyst layer is relatively less, compared with the diffusion layer. The evaporation interface continues to move until it reaches the proton exchange membrane, where the water is primarily in the form of membrane water. Then, the water is transfered to gas flow path and blown away. Given the above analysis, the water transport mechanism of the purging and dewatering process are summarized in table 2.

Table 2. Transmission mechanism of water process

PEMFC components	State of water	Transmission mode
Channel	Liquid water	Convection
Convection diffusion layer	Liquid water	Evaporation and diffusion
Catalyst layer	Liquid water and membrane water	Evaporation and diffusion
Proton exchange membrane	Membrane water	Evaporation

The effectiveness of purging and dewatering process should consider both the amount of water removed and the energy consumption. During this process, the energy consumption caused by air compressor is the highest. The energy consumption of other equipment is too small to be considered. The power calculation of the air compressor is as shown in following.

$$P_{\text{comp}} = 1000 C_{\text{p}} T_{\text{atm}} f \left(P^{\frac{2}{7}} - 1 \right) / \tau \tag{9}$$

Where, C_{p} is the specific heat capacity at constant pressure for air. T_{atm} is the ambient temperature. f is the air flow rate. P is the back pressure of the air compressor. τ is the efficiency of the air compressor. Under a given condition, the purging air flow rate is directly proportional to the power of the air compressor.

As in the process of low-temperature startup, once the water inside the PEMFC freezes, it will cause the volume of the substance to expand. This change leads to the damage of the internal structure and affect the service life. Therefore, the water content inside the PEMFC needs to satisfy the following relationship to ensure a successful low-temperature startup.

$$\lambda_{\text{sum}} > \lambda_{\text{initial}} + \lambda_{\text{generate}} \tag{10}$$

Where, λ_{sum} represents the total water content in the porous structure of PEMFC. λ_{initial} is the initial water content of PEMFC. $\lambda_{\text{generate}}$ is the water content generated by the reaction during the low-temperature startup.

Reducing the initial water content inside PEMFC under shutdown condition is a key factor for successful low-temperature startup. Blowing and dewatering is the primary measure to reduce the initial water content, which makes it a necessary auxiliary measure for low-temperature startup. However, in terms of controlling the amount of water removed, multiple factors, such as blowing flow rate, blowing time and blowing gas temperature, should be considered. This paper primarily examines the impact of the three operational parameters on the water content inside the membrane after blowing.

To conduct the complex analysis, orthogonal experiment and multi-factor analysis of variance are used for the three parameters. Specially, the blowing flow rate is set from 5×10^{-6}kg.s^{-1} to 2×10^{-5}kg.s^{-1}. The blowing time ranges from 30s to 90s. The blowing gas temperature is set from 0°C to 50°C. The dependent variable is the water content inside the membrane. The analysis results are presented in table 3. Results show that within the range of the independent variable parameters, the blowing time has the most significant impact on the water content inside the membrane, followed by the blowing flow rate. While the blowing gas temperature shows the least influence on the water content.

Table 3. Orthogonal results

Parameter name	Quantitative impact	Proportion
Purge flow	0.14269	0.2175
Purge time	0.38871	0.5925
Purge gas temperature	0.1246	0.19
Total	0.656	1

B. Effect of water content in membrane on low temperature startup

A study is conducted to evaluate the impact of initial water content in membrane on the low-temperature startup performance of PEMFC under the ambient temperature of -30°C. The current density, ice volume fraction in cathode catalyst layer and the Membrane Electrode Assembly (MEA) is cathode side are analyzed. Figure 8 illustrates the relationship of current density and ice volume fraction changing with time with different initial water content. The findings indicate that the PEMFC fails to start at low temperatures under the both conditions.

Notably, membrane with a higher initial water content tend to freeze sooner, with the ice volume fraction rapidly reaching unity and the rate of ice volume increase being significantly higher. The reason is that, the saturated non-freezing water transits into the freezing state more quickly due to the higher water content in the membrane. Additionally, a wetter membrane, which has lower resistance to proton and electron transport, leads to higher current density and increase of water production.

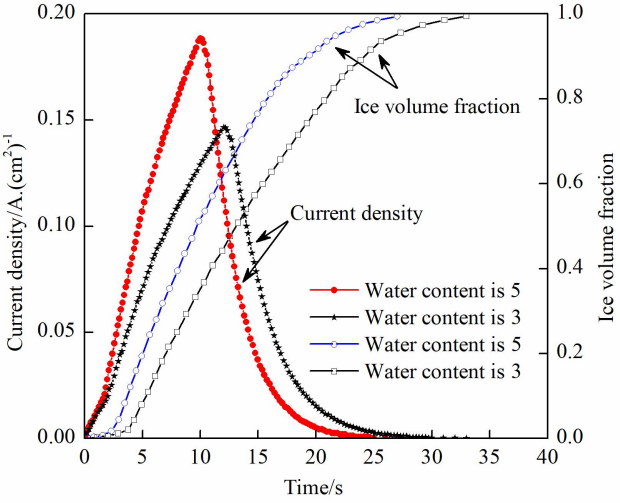

Fig. 8 Current density and ice volume fraction under different initial water content

The dual effects discussed above result in a more substantial accumulation of ice, compared to the condition with lower water content. In the case, where the initial water content is low, the likelihood of successful cold start increases, the time to failure is extended. Therefore, it is advisable to minimize the water content in membrane using effective post-purge and water removal strategies. The purge should balance both the energy consumption and time

constraint.

To further analyze the failure of low-temperature startup under varying operation, figure 9 presents the distribution of ice volume fraction at the cross-section of the middle cathode runner. The results indicate that, the ice coverage remains relatively consistent under two conditions, extending from the diffusion layer to the catalytic layer. Notably, ice formation is less prevalent in the diffusion layer area beneath the flow path. This is primarily caused by the flow of higher-temperature reaction gas through the flow channel. It inhibits ice formation at the interface between the flow channel and the diffusion layer. Moreover, when the water content is set as 5 and the ice volume fraction in cathode diffusion layer exceeds 3, it is observed that this specific water content leads to a rapid increase in current density and enhanced water production in the initial stages. This, in turn, results in the migration of frozen water to the diffusion layer, thus subsequently forming ice.

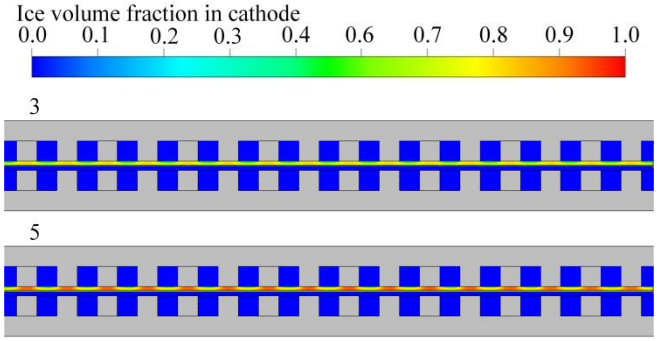

Fig. 9 Distribution of ice volume fraction under different initial water content

C. Effect of temperature on cold start

To reveal the influence of temperature on cold start of PEMFC, the ambient temperatures are set as -30°C, -20°C and -10°C. The water content in membrane is fixed at 3. The changes in current density, ice volume fraction in cathode catalytic layer and ice volume fraction in cathode are obtained as shown in figure 10. The correlation between current density and ice volume fraction is confirmed.

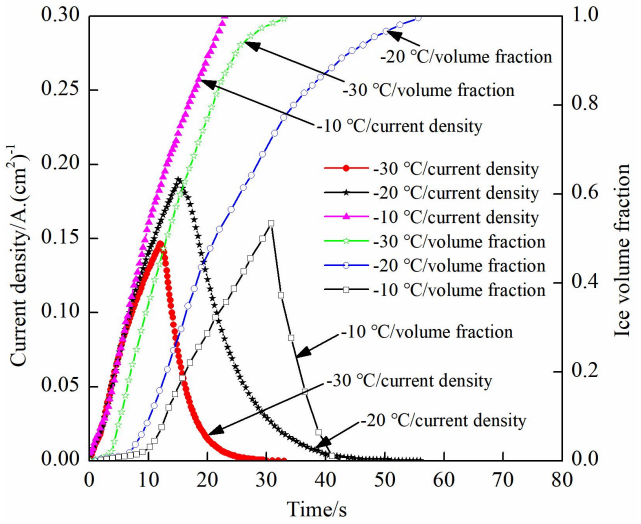

Fig. 10 Current density and ice volume fraction under different temperatures

The results indicate that a successful startup of the PEMFC occurs only at a starting temperature of -10°C. The process is about 32 seconds. In contrast, attempts to start the PEMFC at -30°C and -20°C are unsuccessful. Lower starting temperatures lead to earlier ice formation and a more rapid increase of ice volume fraction within the cathode catalytic layer. The reason is that, as shown in figure 11, the lower temperature accelerates the rate of ice formation, thus in turn diminishes the catalyst activity and reduces current density. Consequently, the generation of both heat and water are decreased. Conversely, higher starting temperatures facilitate a quicker rise in current density, a slower increase in the ice volume fraction within cathode catalytic layer, and a delayed time to reach ice volume fraction of 1. These conditions significantly enhance the likelihood of a successful low-temperature startup.

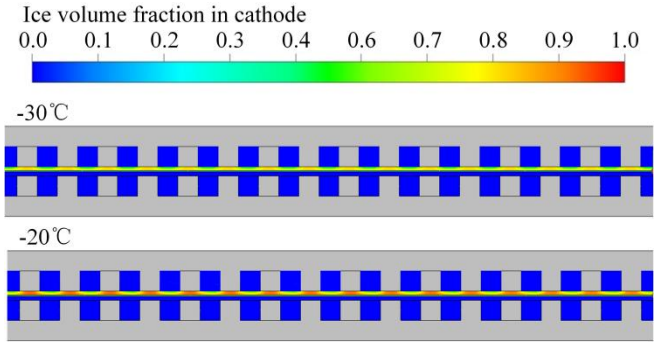

Fig. 11 Distribution of ice volume fraction under different startup temperatures

IV. Analysis of the Influence of Purging on Water Content in Membrane

A. Effect of purge flow on water content in membrane

To confirm the influence of purge flow on water content in membrane, the efficacy of water removal under various shutdown powers are set as 10W, 12.5W and 15W. The range of purge flow rate is selected from 5×10^{-6}kg.s^{-1} to2×10^{-5}kg.s^{-1}. The temperature of purge gas is set as 27°C with a fixed purging time of 90 seconds.

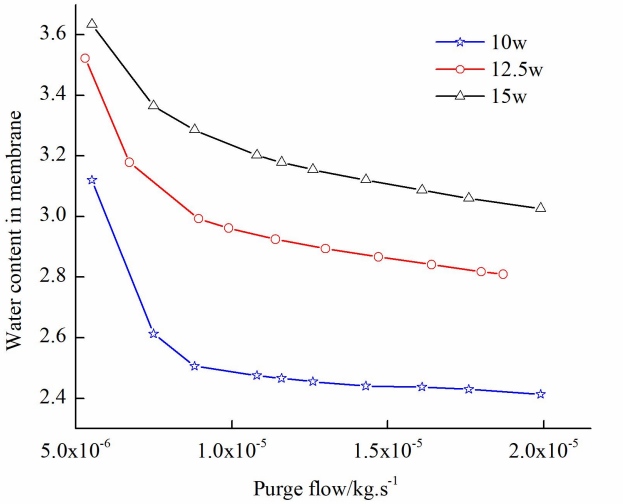

Fig. 12 Relationship between purge flow and water content in membrane under different shutdown power

Results in figure 12 suggest that an increase in purge flow rate leads to a reduce of water content in membrane at the end of the purging process. However, the efficiency of water removal shows a diminishing trend as the purge flow rate increases. The higher the shutdown power, the greater the amount of water produced by PEMFC, subsequently leading

to the increase of water absorption.

Additionally, it is crucial to balance the effectiveness of water removal with the energy consumption associated with purging. Figure 13 illustrates the energy consumption of the compressor under different purging processes. In light of these considerations, to optimize water removal while minimizing energy use, the purge flow rate recommended in this study is 1×10^{-5}kg.s^{-1}. This selection aims to strike an appropriate balance between purging efficiency and operational cost.

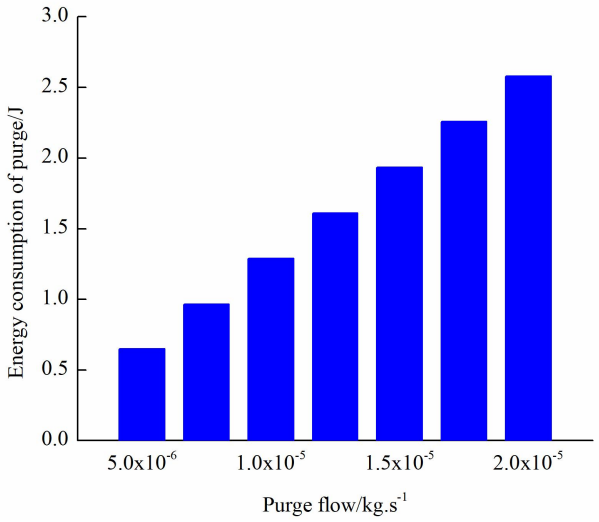

Fig. 13 Variation diagram of purging energy consumption

B. Effect of purge time on water removal efficiency.

To investigate the impact of purge time on water removal efficiency, the purge duration is set from 30 seconds to 90 seconds. The purge flow rate is fixed at 1×10^{-5} kg.s^{-1}. The temperature of the purge gas maintains at 27℃. As shown in figure 14, the results of the effect of purging time on the water content in membrane are given.

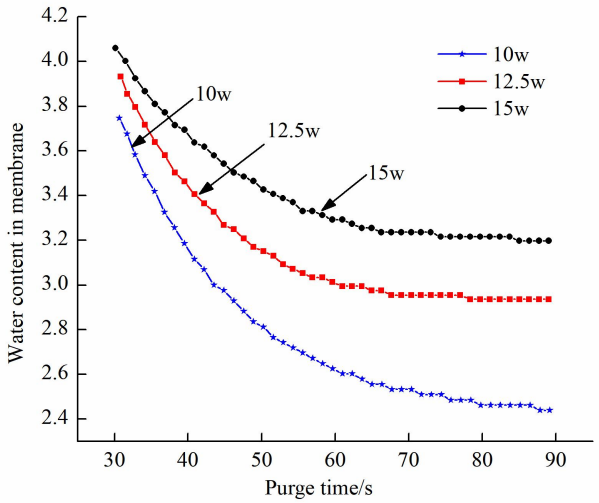

Fig. 14 Relationship between purge time and water content in membrane under different shutdown power

The findings reveal that extending the purge time consistently reduces the water content in membrane under all shutdown powers. Notably, the equilibrium water content is higher at greater shutdown powers. Moreover, the water removal efficiency is more pronounced during the initial 30 to 60 seconds than that in the subsequent 60 to 90 seconds. This pattern suggests that the efficiency of water removal decreases as the purge time lengthens.

Under the three shutdown power settings, the absolute values of the change rate of water content in membrane, that is *K*m, at 60 s are 0.00715, 0.01461 and 0.01743, respectively. For the purposes of this study, any *K*m ≤ 0.01 is used as a criterion to cease purging. Based on this criterion, a purging duration of 56 seconds is selected for the PEMFC operating at a shutdown power of 15W. Thus, the optimal purge time for this specific configuration of the PEMFC is established at 56 seconds.

C. Effect of purge gas temperature on water removal efficiency.

To investigate the impact of purge gas temperature on the efficiency of water removal, the temperature range of the purge gas is set from 0°C to 57°C. Additionally, the purge flow rate is set as 1×10^{-5}kg.s^{-1} with a duration of 90 seconds. Figure 15 depicts the influence of purging gas temperature on the water content in membrane under various shutdown power conditions.

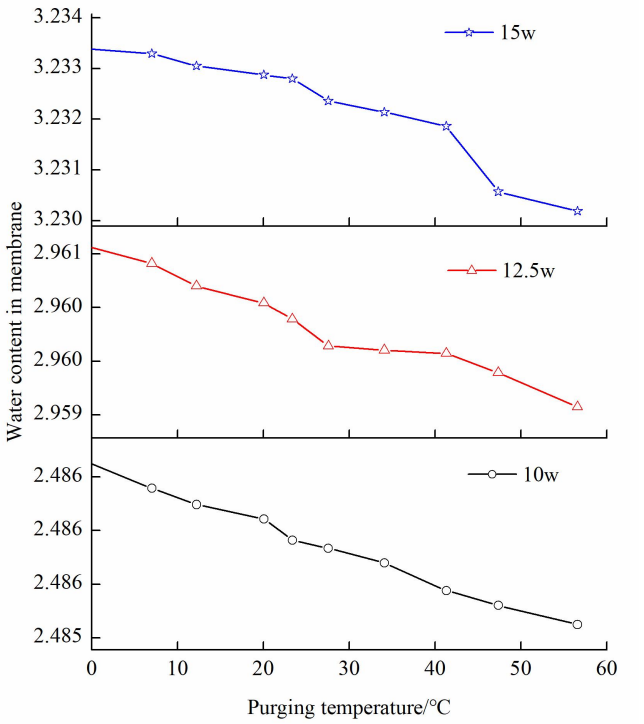

Fig. 15 Relationship of purging temperature and water content in membrane under different shutdown power

The results indicate that variations in purge gas temperature have a minimal impact on the water content of membrane at the end of the purging process, regardless of the shutdown power. However, as the temperature of the purge gas increases, there is a gradual reduction in the water content within the membrane. This effect is more pronounced at higher shutdown powers, where the membrane retains a greater amount of water by the end of the purge. This outcome is attributed to the relatively low temperature of the purge gas compared to the operational temperature of PEMFC at shutdown. Thus, it results in lower saturated vapor pressure and decrease of water removal capability. Consequently, for PEMFC purging, room temperature is an

effective and practical approach.

V. Conclusion

To explore the impact of initial water content within the membrane on the cold-start capabilities of PEMFC under low-temperature conditions, computational fluid dynamics is used. The impact of variations in membrane water content and startup temperature on the low-temperature performance of PEMFC are confirmed. Furthermore, the effectiveness of purge flow rate, purge time and purge gas temperature across various shutdown powers are obtained. The key findings of this study are summarized as followings:

(1) High initial water content in membrane, coupled with low startup temperature, significantly shortens the duration of the startup process. Thus, it increases the likelihood of startup failure of PEMFC.

(2)An increased purge flow rate consistently leads to a reduction in water content of membrane. However, this also leads to a diminished rate of change in water content of membrane. Extending the purge time decreases the water content in the membrane. while, beyond a certain duration, no further significant changes are observed.

(3)Elevating the purge gas temperature tends to reduce the water content in membrane, although the effect of temperature adjustment on water content is minimal. In light of the effects of purging and energy consumption, for the PEMFC studied in this paper, the purging flow rate of 1×10^{-5} $kg.s^{-1}$ and the purging time of 56 seconds are recommended. Ambient temperature for purging gas is the optimal condition for PEMFC.

References

[1] China Society of Automotive Engineering, "Energy Saving and New Energy Vehicle Technology Road-map 2.0," Beijing: China Machine Press, 2020.

[2] Beijing Yiwei New Energy Vehicle Big Data Application Technology Research Center, "China New Energy Vehicle Big Data Research Report," Beijing: China Machine Press, 2021.

[3] Oszcipok M., Zedda M. and Riemann D, "Low temperature operation and influence parameters on the cold start ability of portable PEMFCs," Journal of Power Sources, vol. 154, no.2, pp404-411, 2006.

[4] Montaut A., Moutin S. and Missault D, "Start-up and operation of a 2.5 kW PEMFC System at sub-freezing temperatures," Hydrogen and Fuel Cell Conference, 2009.

[5] C. Li, "Preparation and performance of microporous layers of fuel cell nanofibers." Beijing University of Chemical Technology,2020.

[6] V. VELISALA, "Computational Fluid Dynamics Study of a Compound Flow Field for Proton Exchange Membrane Fuel Cell(PEMFC) Performance Enhancement," Journal of Thermal Science, vol.31, no.6, pp:2374-2384, 2022.

[7] Z. Liao, L. Wei, and D. A, Mohmed, "Numerical study of subfreezing temperature cold start of proton exchange membrane fuel cells with zigzag-channeled flow field," International Journal of Heat and Mass Transfer, vol.165, no. PB, 2021.

[8] Qi. Meng, C. Hao, and B. Yan, "High-performance proton exchange membrane fuel cell with ultra-low loading Pt on vertically aligned carbon nanotubes as integrated catalyst layer," Journal of Energy Chemistry, vol. 71, no. 8, pp:497-506, 2022.

[9] J. Gao, M. Li, and Y. Hu, "Challenges and developments of automotive fuel cell hybrid power system and control," Science China (Information Sciences), vol.62, no.5, pp:50-74, 2019.

[10] T. Chasen, Y. Liang , and X. Xie, "Experimental investigation of liquid water in flow field of proton exchange membrane fuel cell by combining X-ray with EIS technologies," Science China (Technological Sciences), vol.64, no.10, pp:2153-2165, 2021.

[11] T. Yu, "Modeling and optimization of cold start system of fuel cell under low temperature environment," Jilin University, 2023.

[12] S. Lee, S. Kim, and H. Kim, "Water removal characteristics of proton exchange membrane fuel cells using a dry gas purging method," Journal of Power Sources, vol.180, no.2, pp:784-790, 2008.

[13] P. Xu, Y. Gao, and S. Xu, "Purge simulation of proton exchange membrane fuel cell after shutdown," Journal of Tongji University (Natural Science Edition), vol.45, no.12, pp:1873-1878, 2017.

[14] M. Luo, F. Wang, and L. Wei, "PEMFC cold start experiment under secondary purge conditions," Journal of Huazhong University of Science and Technology (Natural Science Edition), vol.39, no.6, 2011.

[15] X. Meng, "Numerical simulation and experimental study on the working process of proton exchange membrane fuel cell (PEMFC)," Guangxi University, 2020.

[16] M. Tang, L. Luo, and W. Chen, "Simulation study on thermal conductivity of bipolar plates in proton exchange membrane fuel cell," Carbon Technology, vol.38, no.5, pp:23-27, 2019.

[17] K. Jiao and X. Li, "Cold start analysis of polymer electrolyte membrane fuel cells," International Journal of Hydrogen Energy, vol.35, no.10, pp: 5077-5094, 2010.

[18] K. Puneet and C. Wang, "Two-phase modeling of gas purge in a polymer electrolyte fuel cell," Journal of Power Sources, vol.183, no.2, pp:609-618, 2008.